European Journal of Pharmaceutics and Biopharmaceutics 203 (2024) 114427

Contents lists available at ScienceDirect

European Journal of Pharmaceutics and Biopharmaceutics

journal homepage: www.elsevier.com/locate/ejpb

Directional freezing and thawing of biologics in drug substance bottles

Sarah S. Peláez [a,b], Hanns-Christian Mahler [a,b,c], Jörg Huwyler [c], Andrea Allmendinger [a,d,*]

[a] ten23 health AG, Mattenstrasse 22, 4058 Basel, Switzerland
[b] Institute of Pharmaceutical Technology, Goethe University Frankfurt, Max-von-Laue-Strasse 9, 60438 Frankfurt am Main, Germany
[c] Department Pharmaceutical Sciences, University of Basel, Klingelbergstrasse 50, 4056 Basel, Switzerland
[d] Institute of Pharmaceutical Sciences, Department of Pharmaceutics, University of Freiburg, Sonnenstr. 5, 79104 Freiburg, Germany

ARTICLE INFO

Keywords:
Biotechnology
Freezing and thawing
Drug substance bottles
Directional freezing
Controlled freezing/thawing
Cryo-concentration
Process characterization
Temperature mapping
Process time

ABSTRACT

Biological drug substance (DS) is typically stored frozen to increase stability. However, freezing and thawing (F/T) of DS can impact product quality and therefore F/T processes need to be controlled. Because active F/T systems for DS bottles are lacking, freezing is often performed uncontrolled in conventional freezers, and thawing at ambient temperature or using water baths.

In this study, we evaluated a novel device for F/T of DS in bottles, which can be operated in conventional freezers, generating a directed air stream around bottles. We characterized the F/T geometry and process performance in comparison to passive F/T using temperature mapping and analysis of concentration gradients. The device was able to better control the F/T process by inducing directional bottom-up F/T. As a result, it reduced cryo-concentration during freezing as well as ice mound formation. However, freezing with the device was dependent on freezer performance, i.e. prolonged process times in a highly loaded freezer were accompanied by increased cryo-concentrations. Thawing was faster compared to without the device, but had no impact on concentration gradients and was slower compared to thawing in a water bath.

High-performance freezers might be required to fully exploit the potential of directional freezing with this device and allow F/T process harmonization and scaling across sites.

1. Introduction

Therapeutic modalities that are classified as biologics such as monoclonal antibodies (mAb), antibody drug conjugates (ADCs), and lately also advanced medicinal products (ATMPS) including nucleic acid-based drug products (DP) and viruses, continue to gain importance for the treatment of sever diseases [1]. Maintaining stability of these complex molecules during manufacturing, storage, transportation, and use remains challenging, yet a key priority and success parameter for these treatments. For the majority of these molecule formats, the drug substance (DS) is typically frozen in bulk before shipment to the fill-finish site to increase storage stability and prolong shelf-life by reducing reaction kinetics, limiting microbial growth of potential bioburden, and to reduce potential interfacial stresses during transportation. Decoupling of DS from DP manufacturing adds flexibility to the manufacturing process and adds significant opportunities with regards to decoupled shelf lives [2]. However, freezing/thawing (F/T) processes are critical unit operations during fill/finish processing, that can impact product quality significantly.

F/T processes are associated with a number of unfavorable conditions that may impact final product quality, especially for proteins. During freezing and thawing, physical instabilities manifesting e.g., as protein aggregates and particles [3,4], and are of major concern as they may impact product quality and safety [5] but may also lead so significant issues in downstream unit operations (e.g., filter clogging) [6].

The physical events that occur during freezing and lead to critical conditions for protein formulations have been previously described in detail [2]. In brief, solutes in a formulation are only partially entrapped in the growing ice during freezing, and thus, solutes in the liquid are transported along with the moving ice front and are eventually

Abbreviations: CQA, Critical quality attribute; CPP, Critical process parameter; DS, Drug substance; DSC, Differential scanning calorimetry; DP, Drug product; EPS, Expandable polystyrene; F/T, Freezing/Thawing; FPF, First point to freeze; FPT, First point to thaw; His, Histidine; LPF, Last point to freeze; LPT, Last point to thaw; mAb, monoclonal antibody; PC, Polycarbonate; PS80, Polysorbate 80; RT, Room temperature; T_f, Freezing point; $T_{g'}$, Glass transition temperature; ULT, Ultra-low temperature.

* Corresponding author at: ten23 health AG, Mattenstrasse 22, 4058 Basel, Switzerland.
E-mail address: andrea.allmendinger@ten23.health (A. Allmendinger).

https://doi.org/10.1016/j.ejpb.2024.114427
Received 16 May 2024; Received in revised form 19 July 2024; Accepted 24 July 2024
Available online 31 July 2024

heterogeneously distributed in the frozen bulk [7]. This is described as the so-called macroscopic cryo-concentration, which will in the following be referred to as cryo-concentration, if not specified differently.

Protein aggregation and sub-visible particle formation after F/T of protein solution has been reported in many cases [3,8–10], and was associated to different stress conditions during F/T. Crystallization of excipients during freezing may lead to a loss of stabilizing effect as it has been reported for example for trehalose and sorbitol [8,10]. Likewise, selective crystallization of buffer system components such a dibasic sodium phosphate or a temperature-dependent shift in pK_a during freezing can lead to a shift in pH, which may result in an increase in protein self-interaction due to differences in the charge heterogeneity profile followed by aggregation [2,11,12]. Also, surface-induced denaturation at the ice-liquid interface has been reported [13,14], whereas the air–liquid interface from air bubbles formed during freezing has been only recently proposed as a potential destabilizing factor [15]. A higher risk for protein oxidation has been also discussed in the context of air bubbles [16]. Most importantly, cryo-concentration can impact protein stability by locally changing protein and excipient concentrations, which may for example lead to an increase in ionic strength [2,3,17]. In particular, the shift of buffer to protein ratio can lead to increased protein self-interaction and consequently destabilization [18]. Cold denaturation of proteins may increase susceptibilities against other freezing induced degradation mechanisms [2,13]. Also, the mechanical stress due to volume expansion of the liquid during freezing, that was observed as significant pressure rise in DS bottles, was proposed as a potential stress during freezing [15,16]. However, the ice-liquid interface and especially the cryo-concentration generated during freezing are considered key factors [19] and especially cryo-concentration promotes several of the above-described critical conditions for protein stability. Both conditions have been directly linked to freezing rates. In fact, slow cooling rates typically lead to a higher degree of cryo-concentration while the resulting specific ice surface area is expected to be smaller, and vice versa for fast cooling rates [2,7].

During the thawing process, freeze-concentrated fractions start to melt and sediment, which leads to a vertical concentration gradient of solutes in the thawed solution [20–22]. These inhomogeneous conditions in solution were shown to destabilize proteins due to a salting out effect at high concentration at the bottom [3,22] or due to self-association effects [23]. Further, slow thawing rates may lead to (re-) crystallization of the liquid [2,24–26].

Overall, previous studies indicate that optimal freezing rates are specific to the protein molecule and formulation, due to molecule specific liabilities [27], while for thawing, faster thawing rates are generally considered less critical [25,26], while care should be taken to not exceed maximum allowable temperatures and holding times.

Besides formulation dependent measures to reduce F/T related stresses to a product (e.g., use of surfactant, cryo-protectants, non-crystallizing excipients, storage below $T_{g'}$ of the formulation), the F/T process needs to be well-characterized selecting optimal process parameters to achieve reproducible F/T processes and thus ensure product quality throughout manufacturing. Controlled F/T processes are therefore preferred.

Currently, there are several technologies available for the pharmaceutical industry to enable controlled freezing and thawing of DS, however, these are typically only available for DS bags. These highly specific F/T systems usually involve high acquisition and implementation costs, both at the DS and the DP site(s), are not interchangeable, and may limit the use to one specific DS container.

In contrast to bags, freezing in DS bottles or carboys is typically conducted by placing the containers into freezer with forced convection (air-blast freezers) or in conventional freezers with stagnant air (without air convection), which is referred to as passive freezing. Even though conventional freezers are not designed to freeze large amounts of liquids [28], in practice they are often used for the same. Passive freezing is dependent on several process parameters, such as the type of freezer, the freezer load, the container size, and the container position in the freezer, etc., which can lead to considerable variability in the process [7,28].

As freezing and thawing of DS is typically performed at different facilities/sites, a controlled and transferrable F/T process is envisaged resulting in constant and reproducible F/T rates independent of equipment properties and process parameters (e.g., container size, the freezer type, freezing temperature, or freezer load). While air-blast freezers, to our knowledge, currently offer the best attempt towards controlled freezing of DS bottles, they are typically not readily available (like ULT freezers) resulting in investment costs.

In this study, we evaluated the impact of a novel F/T device for DS bottles (PharmaTainers™) that intends to better control F/T of DS solution by generating a directed air stream around the bottle. F/T with the device was performed in conventional ULT freezers (for freezing) and at room temperature (RT) (for thawing) and compared to the respective passive F/T process (without use of the device).

First, we studied the device induced F/T geometry by time resolved temperature mapping using a representative surrogate solution for mAbs. We further characterized the device performance at various process conditions by comparing specific time spans calculated from the temperature profiles (i.e., stress times and process times, thawing times), which indicate critical conditions in terms of F/T related stresses. In addition, the extent and distribution of solutes within DS bottles was studied after freezing (ice core sampling) and after thawing (liquid sampling) by measuring concentration gradients of the formulation excipients histidine (His) and polysorbate 80 (PS80), and osmolality. Process conditions comprised different ULT freezer types, different freezer temperatures (−40 °C and −80 °C), different bottle sizes (2L and 5L PharmaTainers™), freezer loads (empty vs. high load by placing ten DS bottles in the freezer) and multiple devices in one freezer (2 devices) to study scalability, different thawing temperatures (2–8 °C and room temperature (RT)), and the comparison to thawing in a water bath.

2. Materials & methods

2.1. Surrogate solution

A 20 mM L-His buffer prepared with L-His (J.T Baker) and L-His HCl (J.T Baker) containing 240 mM sucrose (Pfanstiehl), 10 mM L-Methionine (J.T Baker) and 0.04 % PS80 (J.T Baker) at pH 5.5 was used as surrogate solution for a mAb formulation, which we have previously described as a sensitive model to study cryo-concentration [29]. The solution was sterile filtered using a 0.22 μm PVDF filter (Merck). Sucrose was purchased from Pfanstiehl (Zug, Switzerland), and other chemicals and sterile filters were purchased from VWR (Dietikon. Switzerland). The glass transition temperature ($T_{g'}$) of this surrogate solution was previously determined by differential scanning calorimetry (DSC) to be at −34 °C [29].

2.2. Freeze/thaw (F/T) device and drug substance (DS) containers

The F/T device and 2 L and 5 L polycarbonate (PC) PharmaTainer™ bottles (DS containers), were kindly provided by SaniSure (Camarillo, CA, USA). A schematic drawing of the relevant parts of the device is shown in Fig. 1A. The DS bottle is inserted into an EPS (expandable polystyrene) casing together with four cool packs at each side wall of the rectangular bottle tightly shielding the head space inside the EPS container from the air stream generated by the fan. The packed bottle is placed onto the ventilation unit that generates an air flow directed from underneath the bottle towards the side vents as indicated by the arrows in Fig. 1A. For freezing, the ventilation unit with the packed bottle is placed inside a freezer with the respective target temperature and is connected via a power cable to the controller unit that stays outside the freezer chamber. For thawing, the ventilation unit is placed at a location of respective target thawing temperature, e.g., at RT.

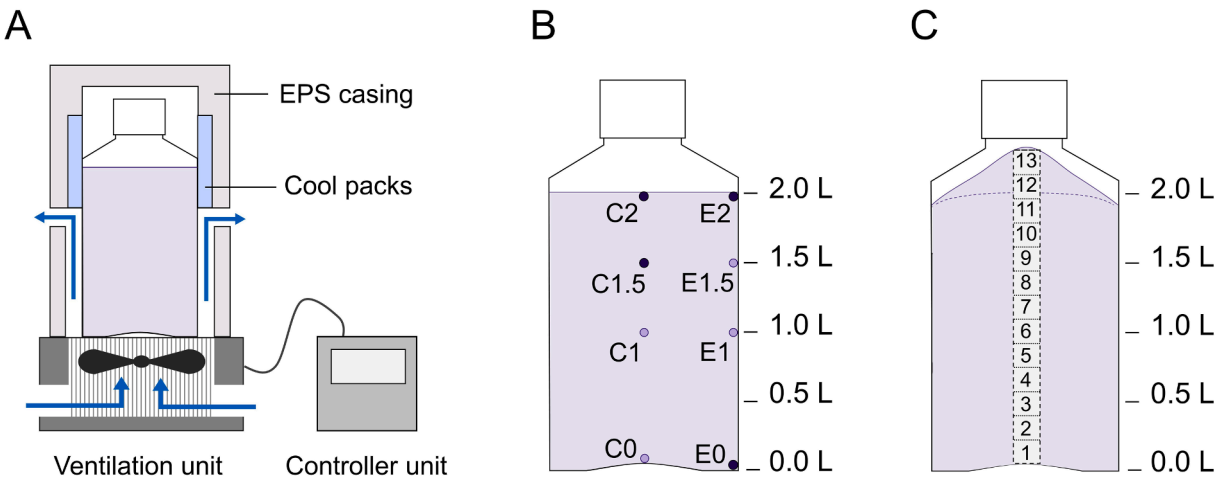

Fig. 1. (A) Schematic drawing of the F/T device consisting of a controller unit and a ventilation unit that holds the EPS casing with the DS bottle inside. The ventilation unit generates a directed bottom-up air flow from as indicated by blue arrows. (B) Positions for temperature monitoring during F/T and sampling after thawing. Positions are labelled with a letter, referring to the radial axis center [C] or edge [E], and a number, referring to the height according to the liquid level indicator on the bottle. Temperature probe positions highlighted as darker dots represent the first point to freeze (FPF), last point to freeze (LPF), first point to thaw (FPT) and apparent last point to thaw (LPT) and were selected after a first temperature mapping experiment, which included all temperature probe positions indicated. (B) Frozen sampling positions along the center axis representing the removed ice core that was cut into slices of 25 mm. The number of ice core samples varied depending on the ice mound present after freezing as indicated.

2.3. Freezing and thawing conditions

Freezing and thawing of the surrogate solution was performed in 2 L and 5 L PC PharmaTainer™ bottles comparing directional F/T when using the device versus non-directional F/T when not using the device (passive F/T). Two independent experimental runs were executed for each condition. Means and standard deviations (SD) were used for data evaluation if not indicated differently.

Freezing experiments were conducted using the following conventional freezers: a −80 °C ULT freezer Revco™ (RDE50086FV) from Thermo Fisher Scientific, (Asheville, NC, USA), referred to as "type 1"; a second type of −80 °C ULT freezer (MDF-U53V) from Sanyo (Osaka, Japan), that has a lower performance (data not shown), below referred to as "type 2"; and a −40 °C low temperature freezer (VF360-45G) from Snijders Labs (Tilburg, Netherlands). The test unit was placed in the center at the bottom of the empty freezer with a consistent door opening time of 1 min before starting the experimental run. Scalability was tested in two set-ups: first, by loading two devices in parallel into the type 1—80 °C freezer, and second, by loading additional ten filled 2 L bottles arranged in a rectangular pattern around the test bottle into the type 1—80 °C freezer (high load set-up).

2.4. Time-resolved temperature mapping

Temperature data during freezing and thawing were acquired using a test set-up as previously described [30]. In brief, an in-house built fixture attached to the bottle was used to place Typ-T thermocouples at defined positions within the liquid. A data logger RDXL6SD-USB from OMEGA Engineering GmbH (Deckenpfronn, Germany) recorded temperature data during freezing and thawing.

First, we evaluated the F/T geometry within the bottles by recording the temperature at eight positions as illustrated in Fig. 1B, four probes were positioned along the edge axis and four along the center axis at heights of liquid level indicators 0.0 L (at the very bottom), 1.0 L, 1.5 L and 2.0 L (at the very top of the liquid level). As a result, four temperature probe positions were selected for further testing to cover the positions at the first point to freeze (FPF) E0, the last point to freeze (LPF) C2 (with the device) or C1.5 (without the device), the first point to thaw (FPT) E0 (with the device) or E2 (without the device), and the apparent last point to thaw (LPT) C2 (with the device) or C1.5 (without the device). The apparent LPT position refers to the position that can be determined from temperature measurements, i.e., the position from which the last piece of ice detaches. As previously described in detail [30], the time point of detachment of ice enables quantification of the approximate thawing time also for conditions at which the absence of ice cannot be determined visually (e.g. when using the device or thawing in the fridge).

2.5. Frozen sampling after freezing

Cryo-concentration after freezing was evaluated using an ice core sampling methodology, which we have previously reported. In this study, we identified the ice core in the radial center (see Fig. 1C) to be indicative (worst case) for studying the cryo-concentration in these DS bottles [29]. In brief, the DS bottle was fixed, the screw cap removed and the first sample on top removed with a stainless-steel corer. Ice core drilling was performed with an electric drill machine (SFS Group, Heerbrugg, Switzerland) equipped with a stainless-steel core dill (ID: 16 mm, OD: 21 mm, length: 200 mm) from Bürkle GmbH (Bad Bellingen, Germany). The sampled ice core was placed on a work surface, cut into 25 mm slices, and each sample transferred into a sample tube for thawing. Samples were numbered starting from the bottom, whereas the number of samples collected (between 11 and 13) was dependent on the ice mound present after freezing (Fig. 1C). The thawed samples were filtered and stored at −80 °C until analysis.

2.6. Liquid sampling after thawing

The concentration gradient in the solution after thawing was evaluated using a liquid sampling setup as previously described by Peláez et al. In brief, liquid samples were collected at relevant positions in the edge at fill heights of 0.0 L (E0), 1.0 L (E1) and 2.0 L (E2) in order to cover highest and lowest concentrations present after thawing as previously reported. Samples of 2.5 mL were collected within 15 min after thawing was completed using a syringe connected to a valve and 300 mm long stainless-steel needle. For sampling, the needle was inserted through a small incision made at the top edge of the bottle. [30].

2.7. Sample analysis

Samples were analyzed for osmolality, PS80 and His concentrations as previously described [29].

In brief, osmolality of the samples was measured by freezing point depression using an Osmomat 3000 instrument from Gonotec. Samples were measured in triplicates and diluted with water if required for analysis.

PS80 was quantified by HPLC-fluorescence micelle assay (FMA) using a Waters Acquity Arc Premier system (Baden, Switzerland) coupled to a waters 2475 fluorescent detector (Baden, Switzerland) according to the method describes by Schmidt et al. [31]. A calibration range between 0.004 % and 0.1 % PS80 was used and samples were diluted with water if required.

His was quantified by a capillary zone electrophoresis (CZE) method using a SCIEX PA800plus system (Brea; USA) with an UV detector and 214 nm filter (SCIEX). A calibration range between 1 mM and 100 mM His was used and samples were diluted with water if required.

Analytical results are presented as concentration factor (CF), which was calculated as ratio of the sample concentration and the initial concentration of the respective surrogate solution used.

2.8. Evaluation of temperature data

Temperature mapping data was quantitatively assessed by calculating different time spans as indicated in Fig. 2. < Process times > for freezing and thawing were defined as the time span between start of the freezing or thawing process < t_{start}>, until the defined target temperature was reached at < t_{end}>, which was for the −80 °C freezers defined to be at −75 °C, for the −40 °C freezer at −39 °C, for thawing at RT at 18 °C, and for thawing in the fridge at 3 °C. The < stress time > was defined as the time between onset of ice nucleation until $T_{g'}$ of the surrogate solution at −34 °C (<t_{glass} >) was reached. This time represents the time span in which the solution is exposed to interfacial stress during ice formation and increasing solute concentration but not yet fully solidified. The onset of ice nucleation was defined as the time where the temperature drops first below 0 °C at < t_{FPF}>, because the actual nucleation time point was not in all freezing conditions clearly detectable. The < thawing time > represents the time span between the start of the thawing process < t_{start} > until the last piece of ice detached from the temperature probe (<t_{melt} >) as indicated by the sharp increase in temperature profiles after the plateau (Fig. 2B). It should be noted that this time span does not include the time for melting of the last piece of ice, which detaches from the temperature probe. This time is negligibly short in our test setups compared to the overall thawing time. We have previously described this phenomenon and its implications for the experimental evaluation of the thawing process in detail, concluding that, whenever possible, thawing times should be determined visually. However, if visual determination is not applicable, as with the device which would require opening the EPS casing, the thawing process should be characterized in advance to ensure that the discrepancy between the time point of detachment of ice from the temperature probe and complete melting is negligible [30].

In order to facilitate the comparison of process benefits of the device, multiplication factors were calculated by dividing the time span required using the device by the time span required when not using the device. A multiplication factor < 1 indicates the device reduced the time span, and > 1 indicates the device prolonged the time span.

Data evaluation and visualization of temperature data was performed with OriginPro, version 2023 (OriginLab Corporation, Northampton, MA, USA.).

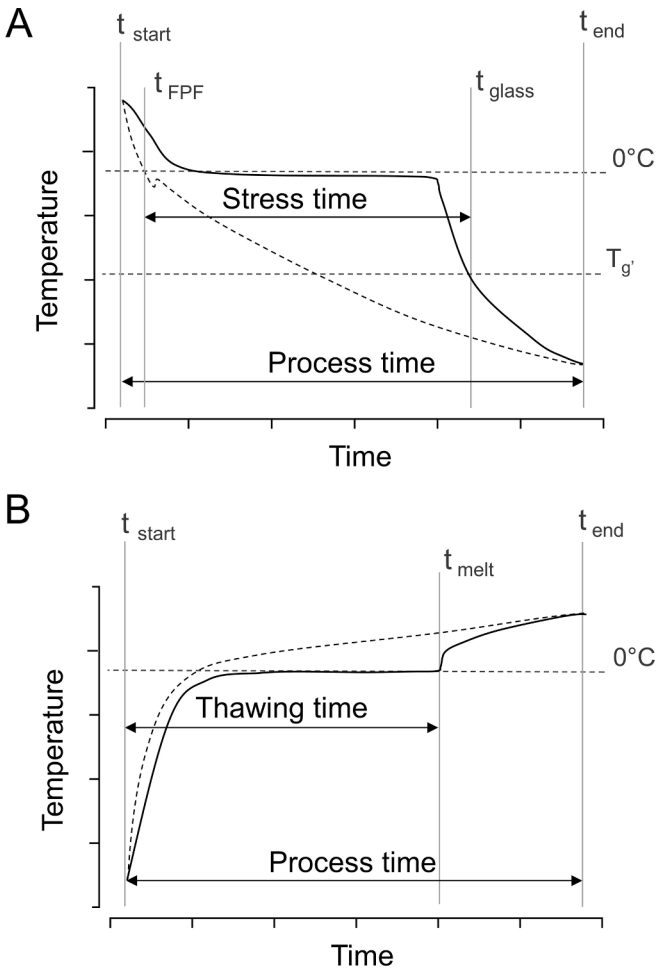

Fig. 2. Exemplary temperature profiles during (A) freezing at the FPF (dashed line) and LPF (solid line) during freezing, and (B) thawing at the FPT (dashed line) and LFT (solid line). Time spans during freezing and thawing were calculated with the indicated reference time points. t_{start}: beginning of the process; t_{FPF}: first point of freezing in the bottle < 0 °C; t_{melt}: last piece of ice detached from temperature probes; t_{glass}: reaching the glass transition temperature ($T_{g'}$) of the of frozen solution; t_{end}: reaching the defined target temperature.

3. Results

3.1. Freezing and thawing front progression

In a first set of experiments, we evaluated freezing and thawing processes in 2 L DS bottles by temperature mapping experiments using a surrogate solution. The temperature mapping revealed the temperature progression in the 2L DS bottles during freezing in a −80 °C freezer and during thawing at RT, referred to as “standard set-up” in the following. Freezing of the solution without the device (passive freezing) in the −80 °C freezer started in the bottom edge, which is the area in contact with the freezer shelf, and after approx. 1 h, freezing started also at the top from the bottle walls (see Fig. 3A). The freezing front progressed from the bottom and from the upper walls towards the LPF, which is for passive freezing in the upper radial center (approximately at position C1.5) as identified from these data, which is also visualized in Fig. 3A after 4 h. In contrast, freezing of the solution with the device occurred predominantly from bottom to top as indicated in Fig. 3B, which we will refer to as directional freezing in the following. At the edge positions along the walls and at half height of the bottle, where the air stream is directed through side vents away from the bottle, temperature decreased faster towards the top, generating a V-shaped freezing front.

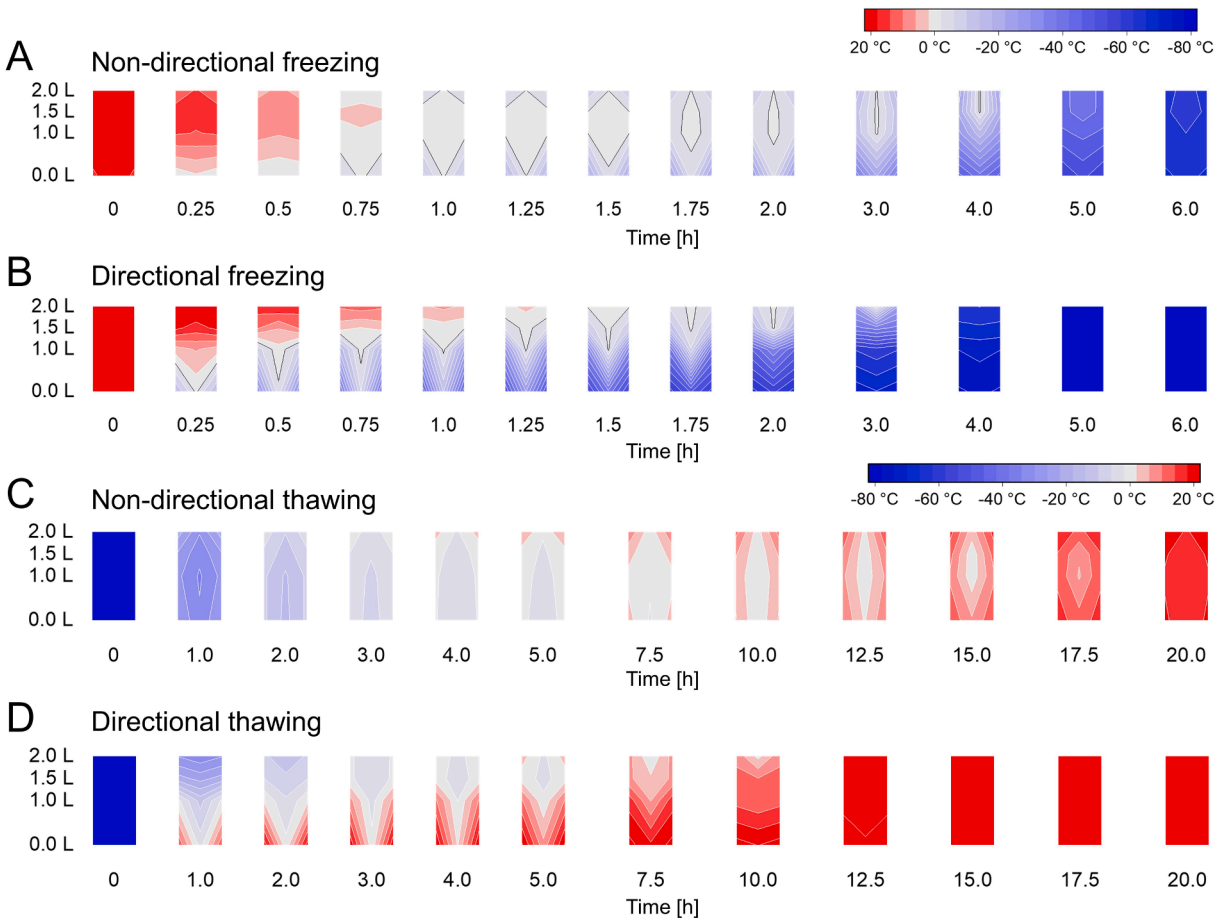

Fig. 3. Exemplary contour plots visualizing the 3D temperature progression dependent on time in hours (h). Isothermal lines reflect temperature gradients from −80 °C to 20 °C. The color transition between blue and red, shown in grey, covers the range between −2°C and + 2 °C to indicate the freezing front progression, and the melting process respectively. (A, B) Temperature progression during freezing in a 2 L bottle over the time course of 6 h in a −80 °C freezer (A) non-directional freezing (without the device) and (B) directional freezing (with the device). The black line indicates the approximate freezing temperature at −2°C to visualize the freezing front progression. (C, D) Temperature progression during thawing of a 2 L bottle during 20 h at RT (C) non-directional thawing (without the device) and (D) directional thawing (with the device).

For the thawing process with the device (Fig. 3D), we report a similar pattern of temperature progression in the bottle with thawing occurring predominantly from bottom to top. Thus, for freezing and thawing with the device, the FPT matches the FPF (position E0), and accordingly the apparent LPT matches the LPF (C2). For thawing without the device at RT (passive thawing), the ice started to melt at the top edges (E2), followed by melting along the walls and then melting of the ice continued towards the center as indicated in Fig. 3C. It must be noted, that unlike for the freezing geometry, the thawing geometry determined by a temperature mapping approach does not reflect the exact thawing geometry due to attachment of ice to the temperature probes during thawing [30], but the data still allows for direct comparison of thawing geometries with or without the device. Based on the results from these initial temperature mapping experiments, we selected four relevant temperature probe positions (i.e., at positions C1.5, C2, E0 and E2) for the following experiments to cover the FPF, LPF, FPT and apparent LPT, for both with and without the device.

3.2. *Device performance at different freezing conditions*

Device performance at different process conditions enabling directional freezing was evaluated by assessing defined time spans (stress and process times) in comparison to the respective passive freezing process (without the device, non-directional freezing). Stress times during freezing are indicative of the extent of freezing stress (ice-liquid surface interaction and cryo-concentration) and process times reflect holding times during drug product manufacturing.

Table 1A summarizes multiplications factors of stress and process times for different tested conditions for directional freezing (when using the device) compared to non-directional freezing (not using the device). Fig. 4 shows the corresponding absolute stress and process times during freezing in hours. For a 2 L bottle in a −80 °C freezer, we determined a reduction in stress time when using the device of 30 % (multiplication factor 0.7), for a 5 L bottle of 50 %, for a 2 L bottle in a different −80 °C freezer (type 2, which had a slightly lower performance) of 20 %, and for a 2 L bottle in a −40 °C freezer of 40 %, respectively. In absolute numbers, the bottles frozen to −40 °C experienced longest stress times (see Fig. 4). For all conditions with a single bottle in the freezer, we elucidated that the device significantly reduced the stress and process time. However, when using two devices in parallel in the −80 °C freezer, multiplication factor increased to 0.9 (reduction in stress time by only 10 %) compared to when freezing of two bottles without the device. In absolute numbers, the stress time was about 1 h longer when using two devices in parallel compared to when using only one device in the −80 °C freezer (standard set-up).

Further, we tested the device performance in a high freezer load set-up by placing 10 additional bottles (without device) in the same −80 °C freezer. In comparison to a 2 L bottle without device, the device even prolonged the stress and process times in the high freezer load set-up i.e., for the stress time from 10.0 h without the device to 12.4 h with the

Table 1
Device performance at different process conditions assessed by multiplication factor of stress and process times for (A) freezing conditions, and thawing and process times for (B) thawing conditions. Multiplication factors were derived by dividing the time span when using the device by the time span without using the device. Time multiplication factors < 1 indicate the time is shortened with the device, and > 1 indicate the time is prolonged with the device.

A

Freezing conditions	Bottle size	Freezer temperature	Freezer type	Freezer load	Multiplication factor of stress time	Multiplication factor of process time
Standard set-up	2 L	−80 °C	type 1	Empty	0.7 (±0.1)	0.6 (±0.1)
Bottle size	**5 L**	−80 °C	type 1	Empty	0.5 (±0.0)	0.4 (±0.0)
Freezer performance	2 L	−80 °C	**type 2**	Empty	0.8 (±0.0)	0.7 (±0.0)
Freezing temperature	2 L	**−40 °C**	–	Empty	0.6 (±0.1)	0.6 (±0.1)
Scalability (2 devices) *	2 L	−80 °C	type 1	**2 devices**	0.9 (±0.0)	0.8 (±0.0)
Scalability (Freezer load)	2 L	−80 °C	type 1	**High load**	1.2 (±0.1)	1.1 (±0.0)

B

Thawing conditions	Bottle size	Freezer temperature	Thawing process	Multiplication factor of thawing time	Multiplication factor of process time
Standard set-up	**2L**	**−80°C**	**RT**	**0.8 (± 0.1)**	**0.7 (± 0.1)**
Bottle size	**5 L**	−80°C	RT	0.4 (± 0.0)	0.4 (± 0.0)
Thawing in fridge	2 L	−80°C	**2-8°C (fridge)**	0.6 (± 0.1)	0.6 (± 0.1)
Freezing temperature	2 L	**−40°C**	RT	0.8 (± 0.1)	0.7 (± 0.1)
Water bath (WB) **	2 L	−80°C	**25°C (Water bath)**	2.9 (± 0.2)	2.7 (± 0.4)

* multiplication factors: 2 device/2 bottles.
** multiplication factors: water bath/device.

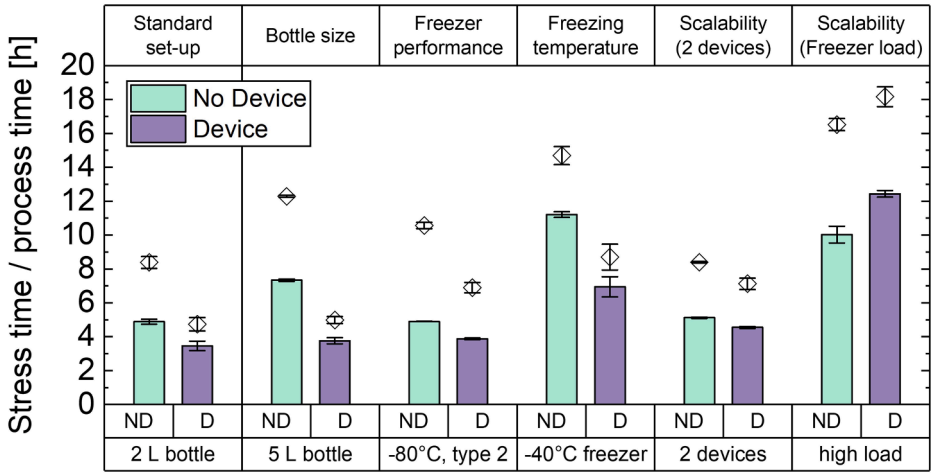

Fig. 4. Device performance for freezing at different process conditions comparing directional freezing (with device [D]) vs. non-directional freezing (without device [ND]). Stress times (bars) and process times (diamond shapes) are shown as means and error bars indicate the standard deviation.

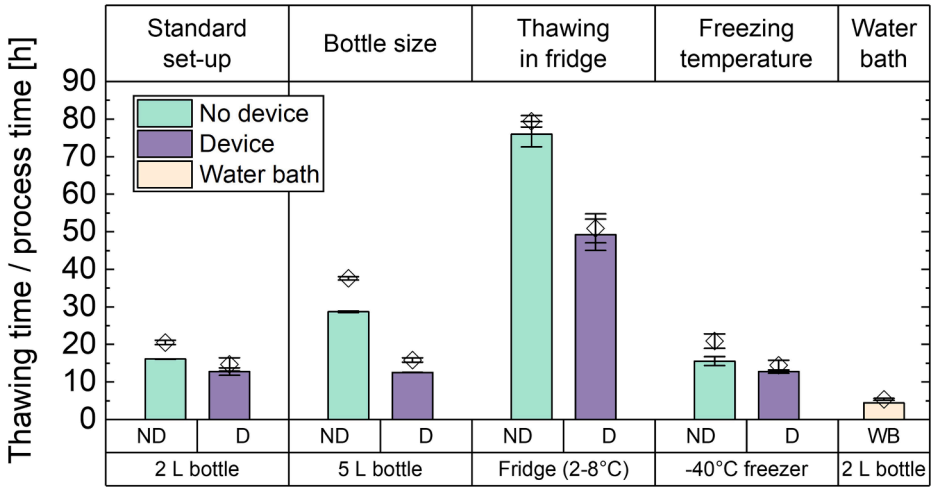

Fig. 5. Device performance for thawing at different process conditions comparing directional thawing (with device [D]) vs. non-directional thawing (without device [ND]). Thawing times (bars) and process times (diamond shapes) are shown as means and error bars indicate the standard deviation.

device (corresponding to a time multiplication factors of 1.2); and for the process time from 16.5 h without the device to 18.2 h with the device (corresponding to a time multiplication factors of 1.1).

Corresponding temperature profiles recorded at the FPF and LPF with use compared to without use of the device for the standard set-up and high freezer load set-up are shown in Fig. 6A and B. As mentioned, the device induced faster freezing in the standard set-up (empty freezer) indicated by a shift in temperature curves to the left. In contrast, in the high freezer load set-up that included 10 additional bottles (Fig. 6B), the device prolonged the process time that was already much longer compared to in an empty freezer. In summary, we demonstrate that the performance of the device was highly dependent on the freezer load.

3.3. Device performance at different thawing conditions

Multiplication factors of stress and process times during thawing are listed in Table 1B for the tested conditions. Fig. 5 shows the corresponding absolute thawing and process times also including the thawing time of a 2 L bottle in a water bath at 25 °C, and Fig. 6C/D shows the corresponding temperature profiles for selected conditions. For all thawing conditions, we found that the device significantly reduced the thawing time and process times compared to passive thawing resulting in a multiplication factor of at least 0.8 (thawing time) and 0.7 (process time) for thawing at RT, for both freezing temperatures tested, −80 °C and −40 °C respectively. For a 5 L bottle, the effect of the device was even larger with a reduction of 60 % for both the thawing time and the process time. The thawing time of a 5 L bottle at RT was about 29 h, and for a 2 L bottle about 16 h. With the device, the thawing time for both bottle sizes was between 12 and 13 h. In comparison, thawing of a 2 L bottle in a water bath was much faster (4.4 h), which corresponds to a time multiplication factor of 2.9 in comparison to thawing with the device. Overall, we conclude that the device significantly reduced thawing and process times for all tested conditions but compared to thawing in a water bath, thawing with the device was slower.

3.4. Cryo-concentration

We further studied cryo-concentration by frozen ice core sampling at two selected conditions in 2 L DS bottles, for the empty −80 °C freezer (standard set-up) and the highly loaded −80 °C freezer (high freezer load set-up) and compared directional freezing (with the device) versus non-directional freezing (without the device) at considerably different freezing rates.

The ice cores post freezing were analyzed for osmolality (Fig. 7A-D), PS80 and His content (Figure A-1 and A-2 in Appendix) and concentration gradients were reported as CFs.

Non-directional freezing of a 2 L bottle without the device in an empty −80 °C freezer led to a concentration of solutes with a continuous increase in concentration towards to bottom (Fig. 7A). The highest concentration (CF 3.8) was found just above the bottom of the bottle and on top in the ice mound region. The lowest concentration factor of 0.6 was found just below the highly concentrated ice mound region.

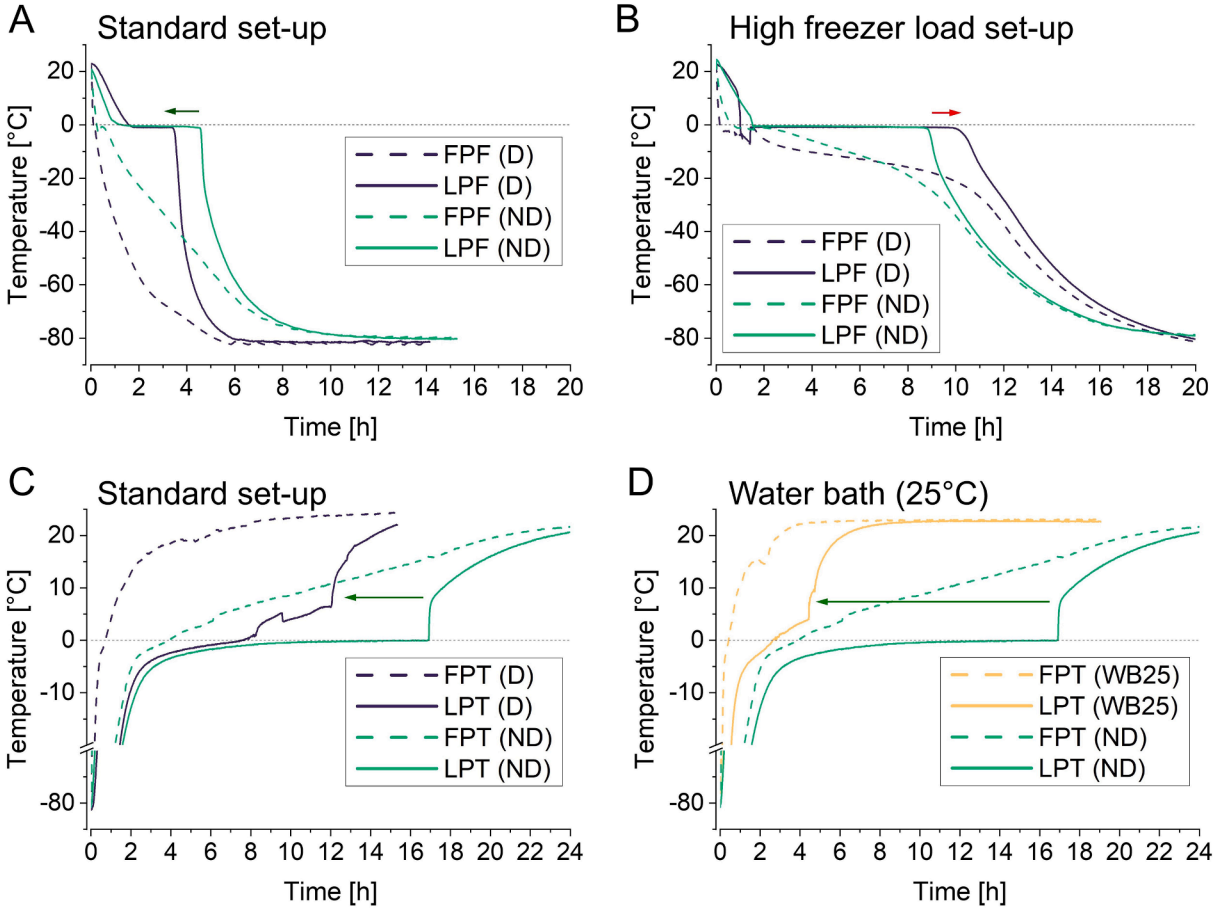

Fig. 6. Representative temperature profiles recorded at the first point of freeze (FPF) and first point of thaw (FPT) (dashed lines) and at the last point of freeze (LPF) and last point of thaw (LPT) (solid lines) to compare F/T during directional freezing when using the device [D] versus not using the device [ND] for (A) standard set-up: freezing of a 2 L bottle in an empty −80 °C freezer; (B) high freezer load set-up: freezing of a 2 L bottle with 10 additional bottles in a −80 °C freezer; (C) thawing in the standard set-up, and (D) thawing in the standard set-up in comparison to thawing in a water bath at 25 °C [WB25]. Arrows indicate the device induced shift in temperature profiles.

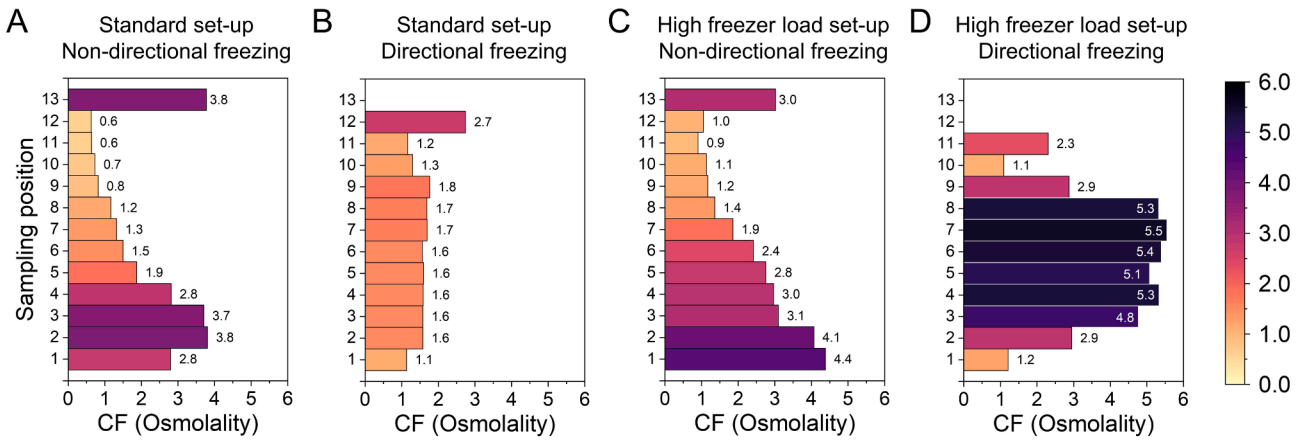

Fig. 7. Cryo-concentrations presented as concentration factors (CF) of osmolality analyzed in ice core samples along the axial center in 2 L bottles after freezing: with the standard set-up (in an empty −80 °C freezer) for (A) non-directional freezing (without device) versus (B) directional freezing (with device); and with the high freezer load set-up (with 10 additional bottles loaded in a −80 °C freezer) for (C) non-directional freezing (without device) versus (D) directional freezing (with device). Bar charts show respective numerical values and are color coded for better visibility.

Directional freezing with the device in an empty −80 °C freezer, which occurred faster compared to passive freezing as discussed above, resulted in a more homogeneous distribution of solutes along the center core and a lower degree of solutes concentration ranging from CFs of 1.1 to 2.7 (Fig. 7B). The highest concentration in the bottle was also found in the top region of the DS bottle.

Non-directional freezing at the high freezer load set-up, which resulted in longer stress and process times and thus slower freezing, led to higher solute concentrations in general, which were particularly high in the lower part of the bottle (Fig. 7C). Both conditions, in an empty (fast freezing) or high freezer load set-up (slow freezing), thus led to a similar solute distribution pattern, with increasing concentrations towards the bottom, but with higher maximum concentration factors of up to CF 4.4 after slow freezing in the high freezer load setup. Similarly, a high concentration was also found in the ice mound region on top of the ice surface for the higher freezer load set-up.

Directional freezing with the device in a highly loaded freezer, which was accompanied by longer process times yielded highest solute concentrations (CFs up to 5.5). The high concentration regions were spread over a wider range in the vertical axis along the center (Fig. 7D). We detected only a small region at the bottom (CF 1.1) as well as below the surface on top (CF 1.2) showing solute concentrations close to the initial concentration.

The cryo-concentration of PS80 and His (Figure A-1 and A-2 in the Appendix) correlated with the osmolality data and we determined the same concentration patterns and comparable CFs in all experiments, while overall PS80 showed marginally lower CFs by trend.

A volume expansion of the liquid towards the top was observed for any process condition (Figure A-3 in Appendix). Bottles that were frozen without the device generated larger ice mounds that appeared as snowy surface with large snow-like crystals present (Figure A-3A and A3-B in Appendix). In contrast, the ice surface in bottles that were frozen with the device appeared as a firm and smooth surface with only little or no ice mound present (Figure A-3C and A-3C in Appendix). Notably, we detected almost no ice mound formation in bottles frozen with the device at the high freezer load set-up that experienced prolonged stress and process times accompanied by highest cryo-concentrations.

3.5. Concentration gradients after thawing

Concentration gradients were further studied after thawing for the standard set-up in three independent experimental runs and liquid samples were collected and analyzed for osmolality, and PS80 and His concentration. Data are presented in appendix (Figure A-4) revealing a vertical concentration gradient after thawing with and without the device, from a high solute concentration at the bottom to a very low solute concentration at the top. In brief, the concentration gradient analyzed at three sampling positions, E0, E1, and E2 when thawed without the device, resulted in osmolality CFs listed from bottom to top of 4.2, 0.7 and 0,1 and with the device of 3.7, 0.4 and 0 respectively. As a result, we did not find substantial differences between concentration gradients observed after thawing with or without the device, i.e. comparing directional and non-directional thawing.

4. Discussion

In this study, we analyzed the impact of directional F/T facilitated by a novel F/T device in comparison to passive processes to better control F/T processes in DS bottles.

Controlling the F/T process is particularly challenging in DS bottles due to the geometrical relationship between surface area and volume (square-cube law) that has direct consequences for the heat transfer leading to high local variabilities in heating/cooling rates within the DS container [16].

In the following section, we first discuss the impact and associated mechanisms of the device-induced directional F/T geometry on process times and cryo-concentration under standard conditions. Second, we elucidate how various process conditions affect the performance of the device (process robustness).

4.1. Device-induced effects on freezing and thawing

The device essentially affected two aspects of the F/T process, (1) the F/T rates in this study quantified as time spans (stress times, thawing times and process times), and (2) the F/T geometry.

4.1.1. Process times

Freezing of a certain amount of liquid is dependent on the temperature gradient and the specific heat capacity of the liquid. The freezing process itself is an exothermal event, which requires removal of latent heat released during crystallization of ice. The Planks equation describes in a simplified way the heat transfer during freezing and has been used to estimate freezing times of DS solutions [16,32]. According to the equation, the freezing process is determined by the container geometry (for a bottle the square dimension), the temperature gradient present between the liquid and temperature outside the bottle (temperature in the freezer), and the heat transfer coefficient. The heat transfer coefficient is substantially different for the following heat transfer

mechanisms listed in order of increasing contribution: natural convection, forced convection and conduction. Active F/T systems for DS bags typically rely on conductive heat transfer through actively temperature-controlled heat transfer surface that are in direct contact with the bags. For DS bottles, air-blast freezers have also been used to generate forced air convection that significantly increases the freezing rate compared to freezers with stagnant air regimes, such as in conventional freezers (passive freezing) [33,34].In our experiments, we studied the effect of forced air convection induced by the air stream from the F/T device, which led in general to faster freezing and thawing. This effect was observed for all tested thawing conditions and for all freezing conditions, in which the cooling capacity of the freezer was not a limiting factor.

The temperature gradient as the other key parameter that drives the freezing process is determined by the temperature in the freezer. Even though conventional freezers have a somewhat limited cooling capacity, they are often used for freezing DS and were therefore also employed in this study.

4.1.2. Freezing geometry: Cryo-concentration

Besides its implications on F/T rates, the device notably changed the F/T geometry. The channeled air stream causes the heat to be dissipated in the same direction, from underneath the bottle along the walls towards approximately half height of the bottle, where the air stream is directed away from the bottle. The upper part of the bottle is shielded from the air stream and surrounded by a head space that effectively insulates it, preventing the liquid from starting to freeze at the surface as observed for passive freezing without the device (Fig. 3).

The induced bottom-up freezing geometry, also described as uni-directional freezing geometry, has been specifically studied in the context of freezing protein solution [15,35,36]. Uni-directional freezing from bottom to top was proposed as beneficial because the ice front is progressing in the opposite direction to the movement of solutes, which are transported downwards due to the density gradient-driven natural convection in the not fully solidified fraction [35]. The time span between nucleation of ice until reaching $T_{g'}$ at the last point in the bottle (stress time) was therefore selected as read-out (see also Fig. 2A) indicating the critical time span for cryo-concentration.

Rodrigues et al. studied the effect of freezing front directions on the resulting cryo-concentration of a bovine hemoglobin solution and showed a major reduction of cryo-concentration for the uni-directional freezing compared to axial freezing caused by reducing natural convection as described above [35]. The concept of uni-directional freezing was also indirectly studied by Duarte et al. with the use of an isothermal cover for DS bottles. In their study, directional freezing in 2 L DS bottles filled with a bovine serum albumin (BSA) solution was “passively” induced by thermally insulating the top part of the bottle, which also resulted in a bottom-up freezing geometry. While only a small reduction of the maximum CF within the bottle was observed, the distribution pattern of BSA changed, and aggregation levels, especially near the top, were lower. [15].

Another important factor that is known to impact cryo-concentration is the ice front morphology. So-called dendritic ice growth has been found to entrap solutes more effectively in the progressing ice front, thereby limiting diffusional and convective movement of solutes and thus reducing cryo-concentration [7,37,38]. Dendritic ice growth was shown to be a function of the freezing rate, i.e., fast freezing favors the formation of ice dendrites [39,40]. For example, Rodrigues and colleagues also mentioned that uni-directional freezing in their set-up contributed to reduced cryo-concentration due to the faster freezing rates achieved, promoting dendritic ice formation. They specifically described that varying freezing rates throughout the bottle, as it is the case for passive (uncontrolled) freezing, may be the major cause for cryo-concentration, due to the absence of dendritic ice in regions that experience slow freezing rates. [41] Thus, because uni-directional freezing is often accompanied by faster freezing rates, it may also effectively reduce cryo-concentration by promoting dendritic ice growth.

Our study confirms that compared to non-directional freezing, the device-induced directional bottom-up freezing effectively reduced the extent of cryo-concentration in our standard set-up (at fast freezing rate) and further led to a more homogeneous distribution pattern of solutes (Fig. 7B).

4.1.3. Freezing geometry: Ice mound formation

A further consequence of the device-induced freezing is that the ice surface appeared smoother and resulted in almost no ice mound as compared to passive freezing. Ice mound formation has been associated with increased internal pressure built-up during freezing [15]; therefore reducing the extent of ice mound formation may also lower the risk of cracks and bursting of bottles. The ice mounds on top of the frozen solution and its implications on protein stability have been recently studied by Duarte et al. using an isothermal cover, which reduced the extent of ice mound formation. For passive freezing, which resulted in pronounced ice mound formation, they found high BSA aggregation levels particularly near the top, which could be prevented by insulating the top using the isothermal cover. The authors attributed the increased aggregation levels near the top to the phenomenon of ice mound formation, which causes the unfrozen solution to be pushed through the air bubble-rich ice structure at the surface, leading to interfacial stress. The foam-like appearance of the resulting ice mound region also indicates increased air-bubble entrapment as described [15]. Hauptmann and colleagues also found higher IgG aggregation levels in the ice mound region at the top, which they explained by an absence of dendritic ice due to slower freezing rates in this region [7], but it may also indicate a potential negative effect of entrapped air bubbles in this top region [16].

In our study, the ice front migration throughout bottles during passive freezing (Fig. 3A) started at the bottom edges where at least some conductive heat transfer is taking place due to contact with the freezer shelf. The freezing front then progresses towards the top in a V-shape because heat is more efficiently dissipated at the walls and following, freezing of the liquid also starts at the top from the edges, eventually entrapping unfrozen solution in the upper center within the ice block. Due to volume expansion of the liquid upon freezing, the remaining unfrozen liquid expands upwards while disrupting the ice surface on top, which causes the frozen material to be piled up forming an ice mound, as previously described [15]. Freezing with the device prevented the liquid from starting to freeze from the top (Fig. 3B), and consequently prevented an extensive ice mound formation and a snow-like (or foam-like) ice surface. Interestingly, using the device without the upper part of the EPS casing indeed also resulted in a pronounced ice mound (data not shown), which confirmed that insulation of the top is a key factor to reduce ice mound formation.

As a result, freezing with the device, which experienced both, an air stream-induced bottom-up directional freezing and insulation of the upper part, overall resulted in lower and more homogeneous distribution of solutes along the radial center, smaller ice mound formation, and the region of highest solute concentration (CF of 2.7) within the bottle was shifted to the top in comparison to passive freezing. This supports the hypothesis that the bottom-up freezing direction limits convection driven cryo-concentration [35] and prevented also in our study a high solute concentration at the bottom center.

4.1.4. Freezing geometry and freezing rate

The question remains, whether the reduced cryo-concentration observed for the standard set-up was primarily due to the directional freezing geometry or the faster freezing rate. To study this effect, the high freezer load set-up was selected to deliberately induce slow freezing rates, which led to prolonged process times. As a result, stress and process times were even longer compared to without the device. At these conditions, while freezing rates were clearly slower, the device still perceived bottom-up freezing in the bottles, which was confirmed by

temperature mapping data. Interestingly, the cryo-concentration was worse for a bottom-up freezing geometry at these slow freezing rates (Fig. 7D), while for non-directional freezing (without the device), with slightly faster freezing rates, the cryo-concentration was not aggravated to this extent (Fig. 7C).

The increased cryo-concentration during bottom-up freezing at slow freezing rates might be caused by both, a lack of dendritic ice growth on a microscopic level as expected due to the slow freezing rates [7,40] and on a macroscopic level by the extended stress times leaving a large portion of the liquid in an unfrozen state and allowing more time for natural convection to promote the concentration along the slow migrating freezing front [35,42].

The stress time, as evaluated from temperature measurements, reflects the time span during which concentration of solutes occurs. A correlation between longer freezing times and a higher degree of cryo-concentration was also reported by several authors [11,19,41]. Minatovicz et al. found that prolonged stress times (referred to as residence time in their study) during freezing of a lactate dehydrogenase (LDH) solution in 1 L DS bottles not only led to a higher extent of cryo-concentrations, but also decreased LDH stability, which they specifically attribute to the increased cryo-concentration-related inhomogeneity [19].

In our study, it is likely that freezing rates were the main driver for cryo-concentration as directional freezing could not predominate this effect. Stress times correlated to the observed extent of cryo-concentrations by trend, which also exemplifies that the stress time is a valuable indicator to predict the expected extent of cryo-concentration.

These findings imply that primarily faster freezing rates may prevent high local solute concentrations, while a bottom-up freezing geometry at fast freezing rates can further increase the macroscopic homogeneity within the bottle, and reduce the formation of ice mounds if freezing at the top is effectively prevented.

4.1.5. Concentration gradients after thawing

After the thawing process, vertical concentration gradients in the thawed solution with a highly diluted region on top and increasing solute concentrations towards the bottom have been previously reported [22,23]. The segregation occurs due to gravity-driven sedimentation of denser freeze-concentrated matrix released from ice mainly consisting of water. The floating ice continuously dilutes the top region until melting is completed [20,22]. After complete thawing, diffusion of solutes towards an initial equilibrium concentration has been shown to be very slow, though faster for small molecules (e.g., His). Consequently, a pronounced concentration gradient of His persistent up until 48 h after thawing as reported in a study by Bluemel et al. [20], a condition that is well known to be critical for protein stability [2,3,22,23]. Thus, the time during which a protein molecule is exposed to these unfavorable conditions should be minimized, and faster thawing can reduce exposure time, but might also reduce the extent of concentration gradients formed in solutions after thawing.

In our study, we pulled liquid samples at different heights (positions E0, E1, E2), immediately after thawing was complete, in order to investigate, whether the faster thawing times achieved by the device will reduce the concentration gradients studied by osmolality, and PS80 and His concentrations (Figure A-4 in Appendix). Even though thawing times were reduced from 16.1 h without the device to 12.8 h with the device, there was no substantial reduction in vertical concentration gradients. Nevertheless, the exposure time and therefore holding time during DP manufacturing was reduced by the shorter thawing times, assuming timely homogenization/mixing of the solution upon complete thawing. In contrast, thawing in a water bath at 25 °C took only 4.4 h in comparison, and thus the exposure times there were even shorter.

4.2. Process robustness and scalability

As mentioned above, freezing and thawing is influenced by the container's geometry, the heat transfer mechanism, and present temperature gradients. The ventilation-induced forced convection of the device in comparison to free convection, as in case of passive F/T, leads to significantly higher heat transfer coefficients, which by theory could be in a range between a 2 to 25-fold increase [28,43]. However, conventional freezers have a limited cooling capacity, as they are not designed to cool down large amounts of liquids. Thus, the rise in temperature in the freezer and the lag time until the target temperature is reached again, leads to a smaller temperature gradient between in and outside of the bottle, that counteracts the effect of the device. As a result, the device's performance is strongly dependent on the freezer's performance. This was not relevant in experiments studying a single unit, meaning the device still clearly reduced freezing times. In case of a fully loaded freezer however, the device's benefit of reducing freezing times was not only diminished by the overloaded freezer, but even prolonged the stress and process times, and even increased cryo-concentration compared to freezing without the device. In our high freezer load set-up when using the device, the stress time was around 2.4 h longer in comparison to freezing at the same set-up without the device, which led to a considerably higher extent of cryo-concentration (Fig. 7C-D). This prolonged stress and process times, also visualized by the shift of temperature curved in Fig. 6B can be explained by the heat that is being generated by the fan itself.

In our thawing process conditions, device performance was not impacted by process conditions, whether it was thawing at ambient temperature or in the fridge. In contrast, thawing in a water bath at the same target temperature was faster, due to the more efficient heat transfer in liquid compared to gas/air.

In summary, freezing with the device could not compensate for a lacking cooling capacity of a freezer. Freezing with the device, especially freezing of multiple units, requires a high-performance freezer to ensure that the benefit of the novel F/T device manifest, i.e., faster freezing leading to shorter stress times and thus reduced cryo-concentration – as it has been shown for a single unit. As a result, the scalability of freezing processes with the novel device using a conventional freezer remains challenging, whereas the thawing process reveals the full potential of the device by reducing associated manufacturing holding times.

4.3. Limitations

In order to be able to conduct a sufficiently large number of experiments, we used a surrogate solution for a mAb formulation including representative formulation compounds and representative solution properties (e.g., $T_{g'}$ of −34 °C, osmolality of 310 mOsmol/kg). The solution was also used in a previously published study where we report the establishment of the ice core sampling methodology specifically optimized to study cryo-concentration in DS bottles. Different analytical read-outs (osmolality, His and PS80 concentration) have been discussed identifying osmolality as a sensitive read-out to investigate cryo-concentration, in combination with the surrogate solution, that has a relatively low viscosity, which reflects a rather worst-case for cryo-concentration, further increasing the sensitivity of this model [29].

To note, the regions within a bottle, where freezing-induced protein aggregation was found varied for different protein molecules and were not necessarily found in regions of high protein concentration, but for example in the top region near the ice mound due to the reasons elaborated above, or at regions with shifted mAb to His ratio [18]. Thus, osmolality is a sensitive read-out to indicate cryo-concentration as a result of a certain F/T protocol without aiming to predict a protein's cryo-concentration, as this would not necessarily indicate protein instability.

The correlation between protein degradation and specific F/T conditions (e.g. F/T rates), process times, stress times, cryo-concentration or ice mounds formed is complex and highly molecule specific beyond the scope and focus of this study. The conditions listed may relevantly impact protein stability and should therefore be characterized and well understood for a certain process.

Whereas this study focused on characterization of the F/T process of a novel device and its implications on cryo-concentration by use of a surrogate solution, a molecule specific assessment is required to study the susceptibility of the molecule to F/T related degradation and the impact on product specific critical quality attributes (CQAs).

5. Conclusion

Controlled F/T processes are used to minimize the impact on product quality and standardizable, scalable processes with low acquisition cost equipment are desired. However, despite air-blast freezers and water baths accelerating process times, active F/T systems for DS bottles with controllable F/T rates are lacking. As a result, F/T is often performed in an uncontrolled manner (passive F/T).

In this regard, we have tested a F/T device and showed that it was able to better control the F/T process by generating a bottom-up directed air stream around the fully insulated bottle resulting in a directional F/T process. We further demonstrated that he F/T front progressed in a V-shape from bottom to top consequently also reducing ice mound formation as a risk for bursting of bottles compared to passive freezing (non-directional freezing). In general, faster freezing and consequently shorter stress times were obtained with the device. We further found that shorter stress times were most likely primarily decisive for reducing the extent of cryo-concentration.

However, we report that the device performance was dependent on the freezer performance and in a fully loaded conventional freezer, the device even prolonged stress times and overall process times urging the need for further improvement or the use in combination with high performance freezers (e.g., air-blast freezer) to allow for scalability and harmonization across manufacturing sites.

Thawing times were per se reduced when using the device compared to passive thawing, and scalability would practically not be limited, especially at RT. However. thawing in a water bath was still much faster (factor 3) compared to thawing with the device. The reduced thawing times did not impact concentration gradients in the liquid and timely homogenization of the solution after thawing is anyways recommended.

Freezing and thawing operations require a thorough process development to identify critical process parameters (CPPs) and their impact on CQAs of the product. We demonstrate that the characterization of F/T processes by temperature mapping and concentration gradients after freezing and thawing using a surrogate solution enhances the understanding of F/T processes in novel equipment configurations and provides data-based rationales to select optimal F/T process setup.

Funding statement

This research was funded by ten23 health and SaniSure.

CRediT authorship contribution statement

Sarah S. Peláez: Writing – original draft, Visualization, Validation, Methodology, Investigation, Formal analysis, Conceptualization. **Hanns-Christian Mahler:** Writing – review & editing, Supervision, Resources. **Jörg Huwyler:** Writing – review & editing. **Andrea Allmendinger:** Writing – review & editing, Supervision, Resources, Project administration, Formal analysis, Conceptualization.

Declaration of competing interest

The authors declare that they have no known competing financial interests or personal relationships that could have appeared to influence the work reported in this paper.

Data availability

Data will be made available on request.

Acknowledgement

We would like to acknowledge SaniSure for providing the PharmaTainer™ bottles and F/T devices. Also, we would like to thank Pau Rubirola Vila, Andrei Hutanu, Steffen Kissing, Katerina Volovecka, Peer Mück, and Evelyn Santos (ten23 health) for supporting analytical method development and testing.

Appendix A. Supplementary material

Supplementary data to this article can be found online at https://doi.org/10.1016/j.ejpb.2024.114427.

References

[1] R. Fang, P. Sane, I. Borges-Sebastiao, B. Bhatnagar, Stresses, Stabilization, and Recent Insights in Freezing of Biologics, in: F. Jameel (Ed.), Principles and Practices of Lyophilization in Product Development and Manufacturing, Springer International Publishing, Cham, 2023, pp. 189–197.
[2] S. Singh, P. Kolhe, W. Wang, S. Nema, Large-scale freezing of biologics —a practitioner's review, part one: fundamental aspects, BioProcess Int 7 (2009) 32–44.
[3] K. Jain, N. Salamat-Miller, K. Taylor, Freeze–thaw characterization process to minimize aggregation and enable drug product manufacturing of protein based therapeutics, Sci. Rep. 11 (2021) 11332.
[4] K. Desai, P. Martin, J. Colandene, W.A. Pruett, D. Nesta, Impact of manufacturing-scale freeze-thaw conditions on a mAb solution, BioPharm. Int. 30 (2017) 30-36-30-36.
[5] C. Thorlaksen, H.S. Schultz, S.K. Gammelgaard, W. Jiskoot, N.S. Hatzakis, F. S. Nielsen, H. Solberg, V. Foderà, C. Bartholdy, M. Groenning, In vitro and in vivo immunogenicity assessment of protein aggregate characteristics, Int. J. Pharm. 631 (2023) 122490.
[6] J.G. Barnard, D. Kahn, D. Cetlin, T.W. Randolph, J.F. Carpenter, Investigations into the fouling mechanism of parvovirus filters during filtration of freeze–thawed mAb drug substance solutions, J. Pharm. Sci. 103 (2014) 890–899.
[7] A. Hauptmann, G. Hoelzl, T. Loerting, Distribution of protein content and number of aggregates in monoclonal antibody formulation after large-scale freezing, AAPS PharmSciTech 20 (2019) 72.
[8] D.M. Piedmonte, C. Summers, A. McAuley, L. Karamujic, G. Ratnaswamy, Sorbitol crystallization can lead to protein aggregation in frozen protein formulations, Pharm Res 24 (2007) 136–146.
[9] S.K. Singh, P. Kolhe, A.P. Mehta, S.C. Chico, A.L. Lary, M. Huang, Frozen state storage instability of a monoclonal antibody: aggregation as a consequence of trehalose crystallization and protein unfolding, Pharm. Res. 28 (2011) 873–885.
[10] B.D. Connolly, L. Le, T.W. Patapoff, M.E.M. Cromwell, J.M.R. Moore, P. Lam, Protein aggregation in frozen trehalose formulations: effects of composition, cooling rate, and storage temperature, J Pharm Sci 104 (2015) 4170–4184.
[11] P. Kolhe, E. Amend, S.K. Singh, Impact of freezing on pH of buffered solutions and consequences for monoclonal antibody aggregation, Biotechnol. Prog. 26 (2010) 727–733.
[12] A. Ukidve, K.B. Rembert, R. Vanipenta, P. Dorion, P. Lafarguette, T. McCoy, A. Saluja, R. Suryanarayanan, S. Patke, Succinate buffer in biologics products: real-world formulation considerations, processing risks and mitigation strategies, J. Pharm. Sci. 112 (2023) 138–147.
[13] A. Arsiccio, J. McCarty, R. Pisano, J.-E. Shea, Heightened cold-denaturation of proteins at the ice-water interface, J. Am. Chem. Soc. 142 (2020) 5722–5730.
[14] B.S. Bhatnagar, M.J. Pikal, R.H. Bogner, Study of the individual contributions of ice formation and freeze-concentration on isothermal stability of lactate dehydrogenase during freezing, J. Pharm. Sci. 97 (2008) 798–814.
[15] A. Duarte, P. Rego, A. Ferreira, P. Dias, V. Geraldes, M.A. Rodrigues, Interfacial Stress and Container Failure During Freezing of Bulk Protein Solutions Can Be Prevented by Local Heating, AAPS PharmSciTech 21 (2020) 251.
[16] J.-R. Authelin, M.A. Rodrigues, S. Tchessalov, S.K. Singh, T. McCoy, S. Wang, E. Shalaev, Freezing of Biologicals Revisited: Scale, Stability, Excipients, and Degradation Stresses, J. Pharm. Sci. 109 (2020) 44–61.

[17] F. Jameel, C. Padala, T.W. Randolph, Strategies for bulk storage and shipment of proteins, Formul. Process Dev. Strateg. Manuf. Biopharm. (2010) 677–704.
[18] O. Bluemel, J.W. Buecheler, A. Hauptmann, G. Hoelzl, K. Bechtold-Peters, W. Friess, The effect of mAb and excipient cryoconcentration on long-term frozen storage stability - part 2: Aggregate formation and oxidation, Int. J. Pharm. X 4 (2022) 100109.
[19] B. Minatovicz, S. Sansare, T. Mehta, R.H. Bogner, B. Chaudhuri, Large-scale freeze-thaw of protein solutions: study of the relative contributions of freeze-concentration and ice surface area on stability of lactate dehydrogenase, J. Pharm. Sci. 112 (2023) 482–491.
[20] O. Bluemel, J.W. Buecheler, A. Hauptmann, G. Hoelzl, K. Bechtold-Peters, W. Friess, Scaling down large-scale thawing of monoclonal antibody solutions: 3D temperature profiles, changes in concentration, and density gradients, Pharm Res 38 (2021) 1977–1989.
[21] P. Kolhe, A. Badkar, Protein and solute distribution in drug substance containers during frozen storage and post-thawing: A tool to understand and define freezing–thawing parameters in biotechnology process development, Biotechnol. Prog. 27 (2011) 494–504.
[22] H. Maity, C. Karkaria, J. Davagnino, Mapping of solution components, pH changes, protein stability and the elimination of protein precipitation during freeze–thawing of fibroblast growth factor 20, Int. J. Pharm. 378 (2009) 122–135.
[23] S.B. Mehta, S. Subramanian, R. D'Mello, C. Brisbane, S. Roy, Effect of protein cryoconcentration and processing conditions on kinetics of dimer formation for a monoclonal antibody: A case study on bioprocessing, Biotechnol. Prog. 35 (2019) e2836.
[24] E. Cao, Y. Chen, Z. Cui, P.R. Foster, Effect of freezing and thawing rates on denaturation of proteins in aqueous solutions, Biotechnol. Bioeng. 82 (2003) 684–690.
[25] A. Hauptmann, K. Podgoršek, D. Kuzman, S. Srčič, G. Hoelzl, T. Loerting, Impact of buffer, protein concentration and sucrose addition on the aggregation and particle formation during freezing and thawing, Pharm. Res. 35 (2018) 101.
[26] N. Rathore, R.S. Rajan, Current perspectives on stability of protein drug products during formulation, fill and finish operations, Biotechnol. Prog. 24 (2008) 504–514.
[27] U. Roessl, S. Leitgeb, B. Nidetzky, Protein freeze concentration and micro-segregation analysed in a temperature-controlled freeze container, Biotechnol. Rep. 6 (2015) 108–111.
[28] J. Johnson, New Approaches For Drug Substance Freezing And Storage, in: Bioprocess Online, 2023.
[29] S.S. Peláez, H.-C. Mahler, P.R. Vila, J. Huwyler, A. Allmendinger, Characterization of freezing processes in drug substance bottles by ice core sampling, AAPS PharmSciTech 25 (2024) 102.
[30] S.S. Peláez, H.-C. Mahler, J. Huwyler, A. Allmendinger, Optimization of methodologies to study freeze/thaw processes in drug substance bottles, Methods and Protocols, in review (2024).
[31] A. Schmidt, A. Koulov, J. Huwyler, H.-C. Mahler, M. Jahn, Stabilizing polysorbate 20 and 80 against oxidative degradation, J. Pharm. Sci. 109 (2020) 1924–1932.
[32] M. Nakach, B. Firas, G. StÉphanie, A. Jean-RenÉ, K. Otmar, B. Cathrin, Freezing time prediction of biologic formulated drug substance using the plank model, PDA J. Pharm. Sci. Technol. 75 (2021) 24.
[33] B. Minatovicz, L. Sun, C. Foran, B. Chaudhuri, C. Tang, M. Shameem, Freeze-concentration of solutes during bulk freezing and its impact on protein stability, J. Drug Delivery Sci. Technol. 58 (2020) 101703.
[34] A. Bezawada, M. Thompson, W. Cui, Use of blast freezers in vaccine manufacture, Bioprocess Int. 9 (2011) 9.
[35] M.A. Rodrigues, G. Balzan, M. Rosa, D. Gomes, E.G. de Azevedo, S.K. Singh, H. A. Matos, V. Geraldes, The importance of heat flow direction for reproducible and homogeneous freezing of bulk protein solutions, Biotechnol Prog 29 (2013) 1212–1221.
[36] M. Rosa, J.M. Tiago, S.K. Singh, V. Geraldes, M.A. Rodrigues, Improving heat transfer at the bottom of vials for consistent freeze drying with unidirectional structured ice, AAPS PharmSciTech 17 (2016) 1049–1059.
[37] S.D. Webb, J.N. Webb, T.G. Hughes, D.F. Sesin, A.C. Kincaid, Freezing biopharmaceuticals using common techniques—and the magnitude of bulk-scale freeze-concentration, BioPharm International 15 (2002) 22–34.
[38] M.F. Butler, Freeze concentration of solutes at the ice/solution interface studied by optical interferometry, Cryst. Growth Des. 2 (2002) 541–548.
[39] M.F. Butler, Instability formation and directional dendritic growth of ice studied by optical interferometry, Cryst. Growth Des. 1 (2001) 213–223.
[40] M.A. Miller, M.A. Rodrigues, M.A. Glass, S.K. Singh, K.P. Johnston, J.A. Maynard, Frozen-state storage stability of a monoclonal antibody: aggregation is impacted by freezing rate and solute distribution, J. Pharm. Sci. 102 (2013) 1194–1208.
[41] M.A. Rodrigues, M.A. Miller, M.A. Glass, S.K. Singh, K.P. Johnston, Effect of freezing rate and dendritic ice formation on concentration profiles of proteins frozen in cylindrical vessels, J. Pharm. Sci. 100 (2011) 1316–1329.
[42] D. Weber, C. Sittig, J. Hubbuch, Impact of freeze–thaw processes on monoclonal antibody platform process development, Biotechnol. Bioeng. 118 (2021) 3914–3925.
[43] P. Kosky, R. Balmer, W. Keat, G. Wise, Chapter 14 - Mechanical Engineering, in: P. Kosky, R. Balmer, W. Keat, G. Wise (Eds.) Exploring Engineering (Fifth Edition), Academic Press, 2021, pp. 317-340.